Diffusion of quercetin in compressed liquid ethyl acetate and ethanol

Bruno Zêzere, João Iglésias, Inês Portugal, José R. B. Gomes and Carlos Manuel Silva*

Department of Chemistry, CICECO – Aveiro Institute of Materials, University of Aveiro, Campus Universitário de Santiago, 3810-193 Aveiro, Portugal

Abstract

Supercritical fluids are alternatives to conventional harmful organic compounds. In the case of supercritical fluid extraction, CO_2 is the most common solvent and can be advantageously modified with small contents of co-solvents like ethanol and ethyl acetate. The rigorous estimation of the tracer diffusion coefficients (D_{12}) of solutes in supercritical mixtures (CO_2 + co-solvent) requires their individual D_{12} values in pure CO_2 and pure co-solvent under the same operating conditions. This essay focuses the diffusivity of quercetin (solute) in two compressed liquid co-solvents (ethanol and ethyl acetate). Quercetin is a natural compound possessing a wide variety of bioactive properties, used as one of the most noticeable dietary antioxidants. The tracer diffusivity measurements are accomplished by the chromatographic peak broadening technique over 303.15-333.15 K and 1-150 bar. The diffusion coefficients lie between 0.4142×10^{-5} and 0.8134×10^{-5} cm^2s^{-1} in ethanol, and between 1.058×10^{-5} and 1.692×10^{-5} cm^2s^{-1} in ethyl acetate. Influence of temperature, pressure and hydrodynamic coordinates is analyzed and discussed based on the most relevant transport theories. Modeling is also carried out with eleven models from the literature and demonstrated the unreliability of predicting equations in opposition to the very good correlations available to fit D_{12} data. The influence of the accurate estimation of auxiliary properties (like

solvent volume and viscosity) upon the calculated tracer diffusivities is also assessed, being possible to detect D_{12} differences as high as ca. 70 %.

Keywords: Quercetin; Ethyl acetate; Ethanol; Diffusion coefficient; Compressed liquid; Modeling

1. Introduction

Quercetin ($C_{15}H_{10}O_7$, Figure 1) is a key dietary antioxidant and an ingredient of medicines and food supplements. This flavonoid is a yellow solid at atmospheric conditions and partially soluble in water and ethanol up to 3.45 mg mL^{-1} [1]. Within its wide variety of bioactive activities, quercetin holds antioxidant [2,3], anti-inflammatory [2], and anti-carcinogenic properties, inhibiting the growth of cells derived from colon [2], breast [4], prostate [5] and stomach [6] cancer. Furthermore, quercetin is also known to prevent coronary heart disease in elderly men [7], as well as osteoporosis and pulmonary diseases [8]. Another interesting feature of this compound is its usage as a reference to determine antioxidant activity [1] and to quantify the flavonoid and carotenoid contents in natural extracts [9–11]. Additionally, quercetin can form complexes with metal ions due to the presence of hydroxyl groups in its aromatic rings (Figure 1). The metal quercetin complexes were found to have a scavenging capacity even better than that displayed by pristine quercetin [3], paving the way for potential clinical applications. For example, a vanadium quercetin complex was shown to weaken mammary cancer [12].

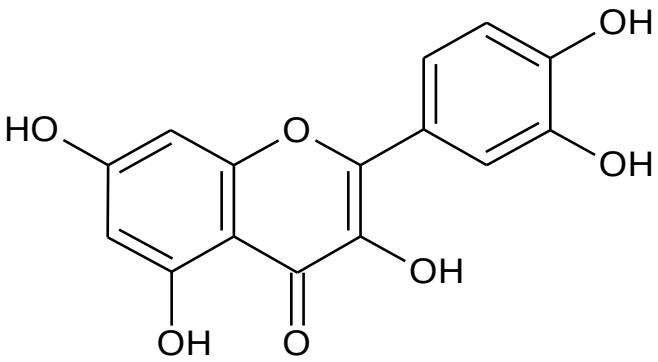

Figure 1 – Quercetin chemical structure.

Quercetin, either in its free form or in the form of glycosides, can be found in many plants such as Chinese herb (*Anoectochilus roxburghii* (Wall.) Lindl.), Ginkgo (*Ginkgo biloba* L.), Persian rose (*Rosa damascena* Mill), onion (*Allium cepa*), watercress (*Nasturtium officinale* R. Br.), apple, and tea (green and black tea leaves) [1,11,13–16]. It was reported in the literature the successful extraction of quercetin from *Ginkgo biloba* L. [15] and *Rosa damascena Mill* [16] using supercritical fluid extraction (SFE) with pure CO_2 or with CO_2 modified with ethanol. The SFE process with a small percentage of the ethanol co-solvent was found to be more effective.

Supercritical fluid extraction is a less harmful alternative to conventional methods carried out with toxic organic solvents [17,18]. The most commonly used solvent is CO_2 due to its intrinsic characteristics, *i.e.*, it is nonflammable, it has a low critical point (304.1 K and 73.8 bar) [19] and can be easily modified with the addition of a co-solvent, which allows for solubility and selectivity enhancement [20]. Among the co-solvents most used in SFE one may cite ethanol (EtOH), methanol [20] and, though not so common, ethyl acetate (EtOAc). For example, the latter has been suggested to be used as modifier in tripterine extraction from *Tripterygium wilfordii*. Hook.f. [21].

With the increasing interest in bioactive compounds from natural sources, for their extraction with green solvents, it is of utmost importance to know transport properties,

such as diffusion coefficients (D_{12}), for accurate design and optimization of industrial equipment and processes. Diffusion coefficient is the property that relates molar flux to chemical potential gradient, hence being of chief importance to mass transfer phenomena. Currently, a lack of both experimental D_{12} values and models for its estimation, especially regarding supercritical mixtures (D_{12}^{mix}), is verified [22]. Accordingly, in this work, the diffusivities of quercetin in compressed liquid ethanol and ethyl acetate are experimentally determined. These solvents were chosen mainly because they are environmentally friendly [23] and are used also as co-solvents for bioactive compounds extraction under supercritical conditions, as mentioned above [20,21]. These measurements are of great importance since the D_{12} values of a solute in pure SC-CO_2 and in the desired co-solvent, (under the same pressure and temperature), can be used to easily estimate D_{12}^{mix}. For this purpose, one can use the Maxwell-Stefan approach [24,25] or, in case of a mixture with small deviations to ideality, the more simple empirical mixing rule of Vignes [26] can be adopted.

2 Theoretical background

2.1 Chromatographic peak broadening technique

The chromatographic peak broadening technique (CPB) is based on the fundamental work developed by Taylor [27–29] and Aris [30]. The method consists in injecting a pulse of a solute in a laminar flow solvent stream in an uncoated cylindrical column; the pulse will then broaden due to the combined effect of convection along the longitudinal axis and molecular diffusion in the radial direction. The concentrations profile at the outlet of the column is given by [31]:

$$\bar{C}(L,t) = \left(\frac{m}{\pi {R_0}^2}\right)\frac{\bar{u}}{\sqrt{4\pi D t}}\exp\left[-\frac{(L-\bar{u}t)^2}{4Dt}\right] \quad (1)$$

where t is the time, L is the length of the column, m is the mass of the solute injected in the column, R_0 is the column inner radius, $\bar{u}$ is the average linear velocity of the solvent, $\bar{C}$ is the radial average solute concentration and

$$D \equiv D_{12} + \frac{R_0^2 \bar{u}^2}{48 D_{12}} \quad (2)$$

Equation 1 can then be fitted to the experimental concentration profile by minimizing the root mean square error, ε, defined as [31,32]:

$$\varepsilon = \left(\frac{\int_{t1}^{t2} \left(C^{\exp}(L,t) - (\bar{C}(L,t)) \right)^2 \mathrm{d}t}{\int_{t1}^{t2} \left(C^{\exp}(L,t) \right)^2 \mathrm{d}t} \right)^{1/2} \quad (3)$$

where t_1 and t_2 are the times at 10 % of the peaks height such that $t_1 < t_2$. Finally, the peaks quality should be evaluated by calculating a series of conditions [31,33–35] as described in detail in previously published works [36,37]: Reynold number (Re) in the laminar flow region; $\mathrm{De}\sqrt{\mathrm{Sc}} < 10$ (De is Dean number and SC is Schmidt number); $D/(\bar{u}L) < 0.01$; $\bar{u}L/D > 0.01$; $\varepsilon < 3$ % and Symmetry factor at 10 % of peak high $(S_{10}) < 1.3$.

2.2 Modeling

Eleven models were tested for the two systems in study: (i) the free-volume model of Dymond-Hildebrand-Batschinski (DHB) [38–40] and its form with the temperature dependence of the minimum diffusion volume (V_D) given by $V_\mathrm{D} = m_\mathrm{VD} T + b_\mathrm{VD}$ [41]; (ii) the hydrodynamic predictive equations of Wilke–Chang [42,43] and Hayduk and Minhas [44]; (iii) the tracer Liu–Silva–Macedo (TLSM) predictive equation and one of its 1-parameter correlations [38,45,46]; (iv) the tracer diffusion correlation for real systems (LJ-1) proposed by Magalhães *et al.* [47]; and (v) four of the empirical and semi-empirical correlations of Magalhães *et al.* [48]. The accuracy of these models was assessed in terms of average absolute relative deviation, (AARD), defined as:

$$\mathrm{AARD}(\%) = \frac{100}{\mathrm{NDP}} \sum_{\mathrm{i=1}}^{\mathrm{NDP}} \frac{D_{12,i}^{\mathrm{calc}} - D_{12,i}^{\mathrm{exp}}}{D_{12,i}^{\mathrm{exp}}} \quad (4)$$

where NDP is the number of points, D_{12}^{calc} is the diffusion coefficient calculated from the models, and D_{12}^{exp} is the experimental diffusivity.

2.3 Properties estimation

Ethanol density was calculated by the Tait [49] and the Eykman [50,51] equations wile viscosity was obtained by the Mamedov equation as suggested by Cano-Gómez *et al*. [52]. The ethyl acetate density was calculated by the Tait equation [49] and by a modified form the Rackett equation [53]. Viscosity values were either taken from Viswanath *et al*. [54] or estimated by the Lucas method [55] when not available, at high pressure. Regarding the critical temperature, pressure and volume (T_c, P_c and V_c respectively), their values were taken from Yaws [53] and Poling *et al.* [43], or estimated through the Joback's method [43,56,57] when not available. The Lennard-Jones molecular diameter (σ_{LJ}) and energy ($\varepsilon_{\mathrm{LJ}}/k_{\mathrm{B}}$) were taken from Liu and Silva [38], or estimated with Equations 7 and 8 from Liu *et al.* [45] when not available.

3 Materials and methods

3.1 Chemicals

Quercetin, ($\mathrm{C_{15}H_{10}O_7}$, CAS number 117-39-5, purity of ≥95 wt.%) was purchased from Sigma-Aldrich, ethyl acetate ($\mathrm{C_4H_8O_2}$, CAS number 117-39-5, purity 99.9 wt.%) from VWR Chemicals, and ethanol absolute anhydrous, ($\mathrm{C_2H_5OH}$, CAS number 64-17-5, purity 99.9 wt.%) from Carlo Erba. All chemicals were used without further purification.

3.2 Experimental conditions

A scheme of the experimental apparatus is shown and described in detail in a previous publication [58]. The procedure consists in pumping the solvent (ethyl acetate or ethanol)

from the reservoir at constant flow rate using a syringe pump. The solvent is then pre-heated in a stainless-steel column placed inside an oven, and fed to an open capillary column (PEEK tubing, $R_0 = 0.261$ mm, $L = 11.182$ m, and $R_c = 0.150$ m) connected to a UV-Vis detector set at a specific wavelength for each solvent. After reaching steady-state conditions (*i.e.*, constant pressure, temperature and baseline) 1–2 h after start-up, a small volume of solute (0.1 μL) is injected in a short period (pulse input). The system pressure is controlled by a back pressure regulator.

The diffusion coefficients of quercetin were measured in pure liquid ethanol and ethyl acetate. The measurements were carried out at temperatures of 303.15, 313.15, 323.15 and 333.15 K, pressures of 1, 50, 100 and 150 bar, flowrate of 0.150 mL min^{-1}, and wavelengths and concentrations values of 245 nm and 2.37 mg mL^{-1} for ethanol and 270 nm and 0.63 mg mL^{-1} for ethyl acetate (see section 4.1). The wavelength and concentration values were established by analyzing the range 205 – 405 nm and 0.21 – 2.37 mg mL^{-1} (etanol) and 250 – 400 nm and 0.37 – 1.25 mg mL^{-1} (ethyl acetate).

4 Results

4.1 Wavelength and concentration study CPB method validation

Before performing the D_{12} measurements, the concentration of the solute to be injected and the wavelength at which the signal is to be recorded had to be optimized for quercetin in both solvents. The concentration optimization consisted in finding a value that could guarantee infinite dilution and also a peak high enough in order to obtain reliable D_{12} values. The wavelength should be selected in order to ensure signal linearity, low ε and high D_{12} reproducibility [31,59]. The preliminary assays were carried out at 323.15 K and 1 bar for both systems, at wavelengths intervals of 205 – 405 nm and 250 – 400 nm, with

concentrations values between 0.21 and 2.37 $\mathrm{mg\,mL^{-1}}$ and between 0.37 and 1.25 $\mathrm{mg\,mL^{-1}}$ for EtOH/quercetin and EtOAc/quercetin, respectively. Ultimately, the determined optimal wavelength and concentrations were 245 nm and $2.37\ \mathrm{mg\,mL^{-1}}$ for EtOH/quercetin (Figure 2 (a), (c) and (e)) and 270 nm and $0.63\ \mathrm{mg\,mL^{-1}}$ for EtOAc/quercetin (Figure 2 (b), (d) and (f)). These conditions ensured high reproducibility, signal linearity and low ε for both systems. In addition, infinite dilution was ensured by injecting 0.1 µL of solution per assay, which corresponds to inject only 7.84×10^{-4} and 2.1×10^{-4} µmol of quercetin in ethanol and ethyl acetate, respectively. These values are in accordance with data reported in the literature, e.g. for α-pinene (6.17×10^{-4} µmol) [60], $\mathrm{Ni(acac)_2}$ (5.01×10^{-4} µmol) and $\mathrm{Pd(acac)_2}$ (4.02×10^{-3} µmol) in ethanol [58].

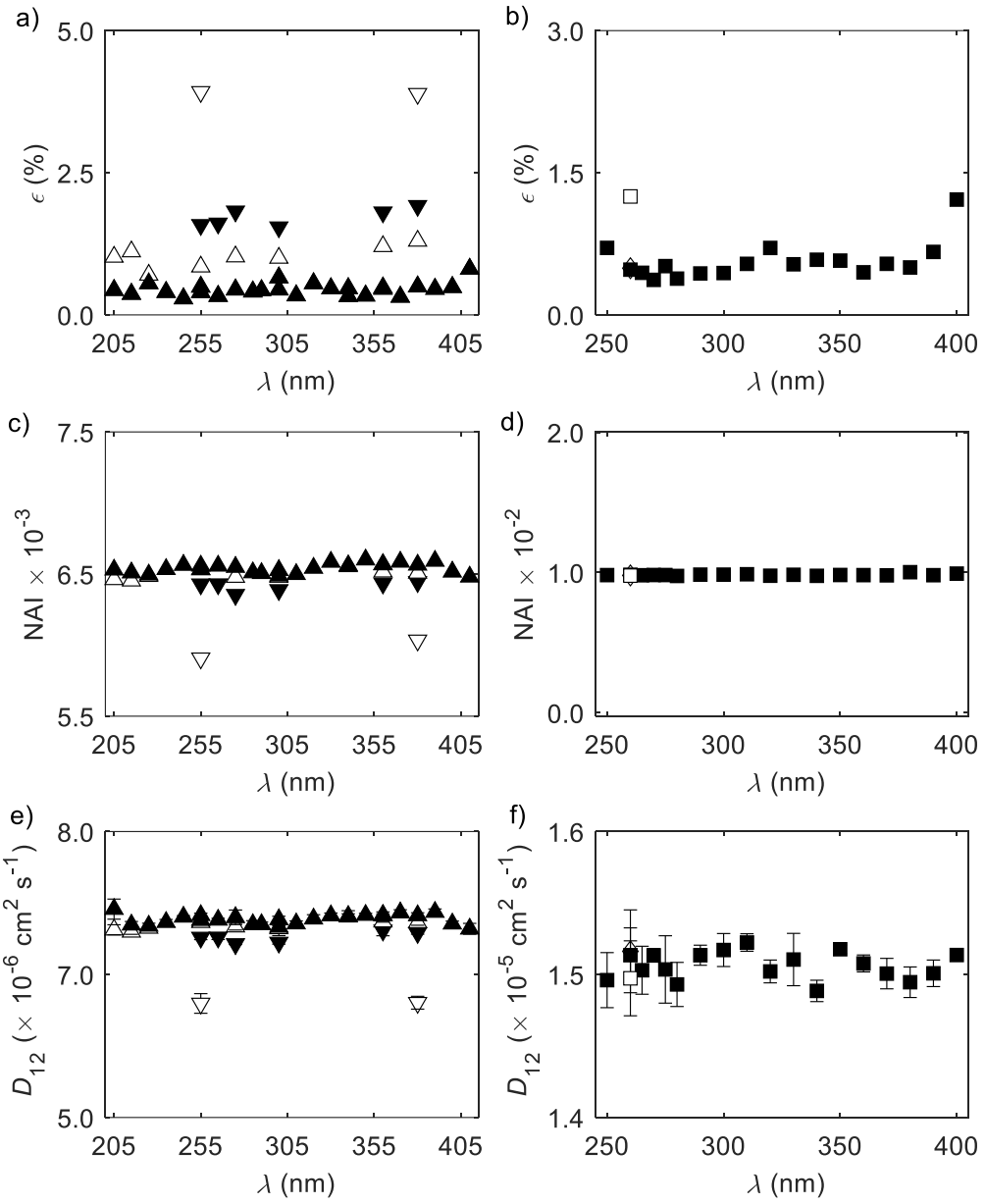

168

169 Figure 2 – Determination of the optimal detector wavelength (λ) for EtOH/quercetin and EtOAc/quercetin at 1 bar and
170 323.15 K. In the case of EtOH/quercetin: (a) Root mean square error, ε (c) Ratio of maximum absorbance to peak area
171 (NAI $= \mathrm{Abs_{max}}/\mathrm{A_{peak}}$) (e) Preliminary D_{12} results for ▲ $= 2.37$ mg mL^{-1} , △$= 1.36$ mg mL^{-1} , ▼$=$
172 0.68 mg mL^{-1} , ▽$= 0.21$ mg mL^{-1}. In the case of EtOAc/quercetin: (b) ε (d) NAI (f) Preliminary D_{12} for □ $=$
173 1.25 mg mL^{-1}, ■ $= 0.63$ mg mL^{-1} ◇ $= 0.37$ mg mL^{-1}.

174 The applicability of the CPB method was ensured in both systems. For EtOH/quercetin:
175 (i) Re ranged from 4.31 to 7.96, obeying laminar flow; (ii) $\bar{u}$ from 1.13 to 1.18 cm s^{-1};

(iii) $D/(\bar{u}L) < 0.01$, guarantying concentration profiles with approximate Gaussian form; (iv) negligible secondary flow effects inside the column, *i.e.* De$\sqrt{\text{Sc}}$ <10, where De and Sc are the Dean and Schmidt number respectively; (v) temperature and pressure perturbations are neglected, *i.e.* $\bar{u}L/D > 1000$; (vi) a peak presents a good fitting $\varepsilon \leq 0.85$ %; and (vii) asymmetry, S_{10}, between 1.16 and 1.23. For quercetin in ethyl acetate: (i) Re ranged from 11.55 to 18.16; (ii) $\bar{u}$ from 1.14 to 1.21 cm s^{-1}; (iii) $D/(\bar{u}L) < 0.01$; (iv) De$\sqrt{\text{Sc}}$ <10; (v) $\bar{u}L/D > 1000$; (vi) $\varepsilon \leq 0.69$ %; and (vii) $S_{10} \cong 1$. For these restrictions to be evaluated it was necessary to previously calculate both solvent density and viscosity.

4.2 Measured diffusion coefficients of quercetin

The values of D_{12} obtained for quercetin in ethanol are presented in Table 1 alongside the calculated values of density, viscosity and molar volume. For quercetin in ethyl acetate equivalent results are shown in Table 2. A graphical representation for both systems can be seen in Figure 3.

Table 1 – Experimental D_{12} values for quercetin in ethanol and calculated density (ρ_1), viscosity (μ_1) and molar volume (V_1) of the solvent.

Temperature (K)	Pressure (bar)	$D_{12} \pm \Delta D_{12}$ (10^{-5} cm^2 s^{-1})	ρ_1 (g cm^{-3})	μ_1 (cP)	V_1 (cm^{3}mol^{-1})
303.15	1	0.4589 ± 0.0027	0.7820	0.9650	58.91
	50	0.4432 ± 0.0014	0.7858	1.007	58.63
	100	0.4268 ± 0.0005	0.7899	1.049	58.33
	150	0.4142 ± 0.0015	0.7937	1.090	58.04
313.15	1	0.5636 ± 0.0028	0.7730	0.8100	59.60
	50	0.5422 ± 0.0021	0.7774	0.8478	59.26

	100	0.5216 ± 0.0008	0.7817	0.8854	58.94
	150	0.5093 ± 0.0037	0.7857	0.9221	58.63
323.15	1	0.6807 ± 0.0017	0.7640	0.6870	60.30
	50	0.6533 ± 0.0007	0.7690	0.7209	59.91
	100	0.6338 ± 0.0022	0.7735	0.7547	59.56
	150	0.6156 ± 0.0033	0.7777	0.7876	59.24
333.15	1	0.8134 ± 0.0058	0.7560	0.5870	60.94
	50	0.7786 ± 0.0037	0.7606	0.6179	60.57
	100	0.7556 ± 0.0047	0.7652	0.6484	60.21
	150	0.7371 ± 0.0018	0.7696	0.6780	59.87

[i]Density estimated by Tait [49] and the Eykman [50,51] methods and viscosity by the Mamedov equation [52].

Table 2 – Experimental D_{12} values for quercetin in ethyl acetate and calculated density (ρ_1), viscosity (μ_1) and molar volume (V_1) of the solvent.

Temperature (K)	Pressure (bar)	$D_{12} \pm \Delta D_{12}$ (10^{-5} cm^2 s^{-1})	ρ_1 (g cm^{-3})	μ_1 (cP)	V_1 (cm^{3}mol^{-1})
303.15	1	1.152 ± 0.005	0.8877	0.3994	99.26
	50	1.133 ± 0.004	0.8920	0.4223	98.78
	100	1.103 ± 0.002	0.8970	0.4439	98.23
	150	1.058 ± 0.003	0.9010	0.4644	97.79
313.15	1	1.319 ± 0.007	0.8756	0.3590	100.6
	50	1.283 ± 0.010	0.8810	0.3802	100.0
	100	1.261 ± 0.004	0.8850	0.4003	99.56
	150	1.209 ± 0.009	0.8900	0.4193	99.00

323.15	1	1.513 ± 0.005	0.8634	0.3247	102.1
	50	1.439 ± 0.008	0.8690	0.3444	101.4
	100	1.425 ± 0.007	0.8738	0.3632	100.8
	150	1.377 ± 0.004	0.8780	0.3810	100.4
333.15	1	1.692 ± 0.005	0.8508	0.2952	103.6
	50	1.642 ± 0.006	0.8560	0.3138	102.9
	100	1.591 ± 0.002	0.8610	0.3315	102.3
	150	1.533 ± 0.008	0.8670	0.3484	101.6

[i]Density estimated by Tait equation [49] and a modified form the Rackett equation [53] and viscosity taken from [54] or estimated by the Lucas method [55].

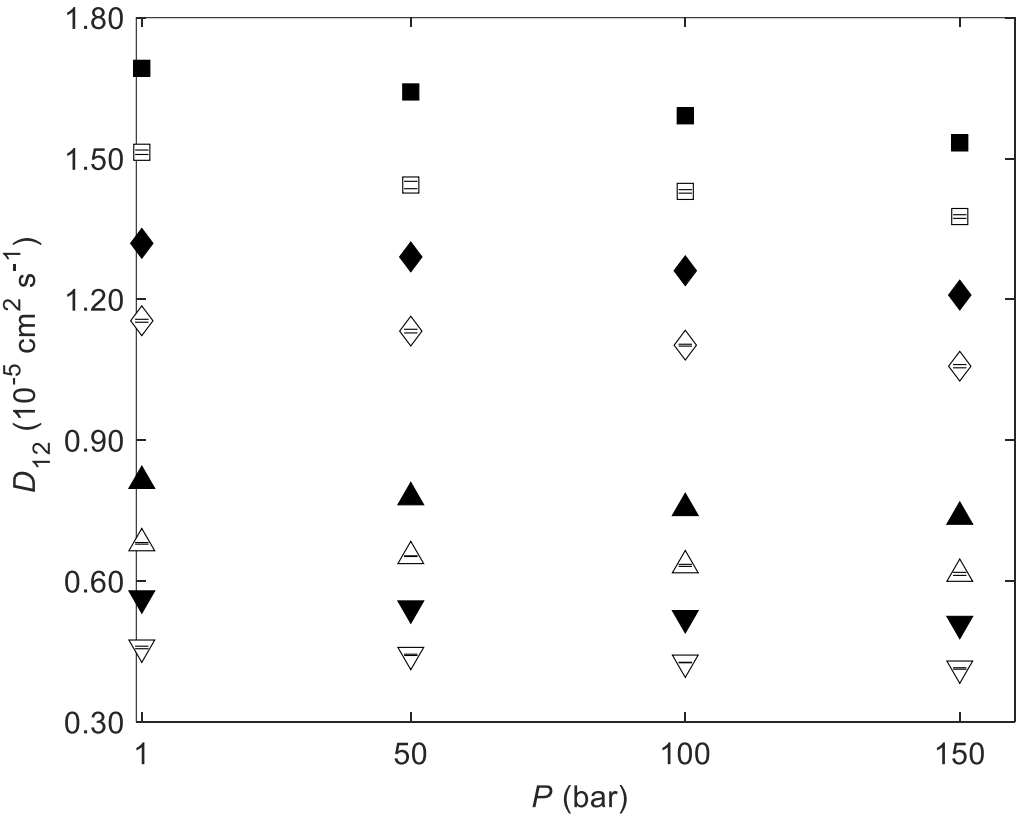

Figure 3 – D_{12} values *versus* P pressure for quercetin in compressed liquid ethanol (▲. △, ▼ and ▽) and in compressed liquid ethyl acetate (■, □, ◆ and ◇) for temperatures of 303.15 K (▽ and ◇), 313.15 K (▼ and ◆), 323.15 K (△ and □) and 333.15 K (■ and ▲).

By comparing Tables 1 and 2 and by observing Figure 3 it is clear that the D_{12} values of quercetin in ethyl acetate are higher than those in ethanol. This difference can be explained by two main reasons: (i) ethanol is far more polar than ethyl acetate, which allows the quercetin molecules to establish stronger intermolecular forces with ethanol, and thus to diffuse more easily in ethyl acetate**;** (ii) in terms of free-volume theory, ethyl acetate exhibits higher free volume ($V_{\mathrm{f}} = V_1 - V_{\mathrm{D}}$) than ethanol, meaning that the solute has more space to move through the first solvent [61]. Parameter V_{D} (minimum free volume required for diffusion) is obtained from the DHB correlation, which we will discuss further in section 4.3.

Analysing now the trends found within each system, as expected, increasing the pressure leads to a decrease of D_{12} while increasing the temperature leads to an increase of D_{12}, as found in other studies [32,58,60]. The first trend can be justified by the fact that with the increasing of pressure the free volume of the solvent decreases. Furthermore, as the solvent molecules become more packed, more energy is required for the solute to escape from the force field generated by the solvent, penalizing its diffusion [61–63]. Regarding temperature effects, with its increase, the internal energy of the system also increases, which facilitates diffusion.

Diffusion was also analyzed as a function of common Stokes-Einstein abscissas (T/μ_1). By observing Figure 4 one can conclude that the linearity of the EtOH/quercetin system is far superior than that of the EtOAc/quercetin. In fact, this can be quantified by calculating the coefficient of determination, R^2, for the linear fit of D_{12} and T/μ_1. The first system achieves $R^2 = 0.996$ while the last one provides a lower value of $R^2 = 0.974$. Furthermore, in both systems a small deviation is present at the y-intercept, taking values of $1.878 \times 10^{-7}\ \mathrm{cm^2 s^{-1}}$ for the EtOH/quercetin system and $1.364 \times 10^{-6}\ \mathrm{cm^2 s^{-1}}$ for EtOAc/quercetin. This finding is consistent with previous works

dealing with this subject [41,64]. Another observation is the similar trend exhibited by the four sets of four points in Figures 4 (a) and (b), where parallel straight lines could correlate the results with temperature-dependent y-intercepts. In the whole, those results show that mass transport in compressed liquids is not accurately interpreted by simple hydrodynamic theories, which means some modification or correction must be introduced in order to improve their performance.

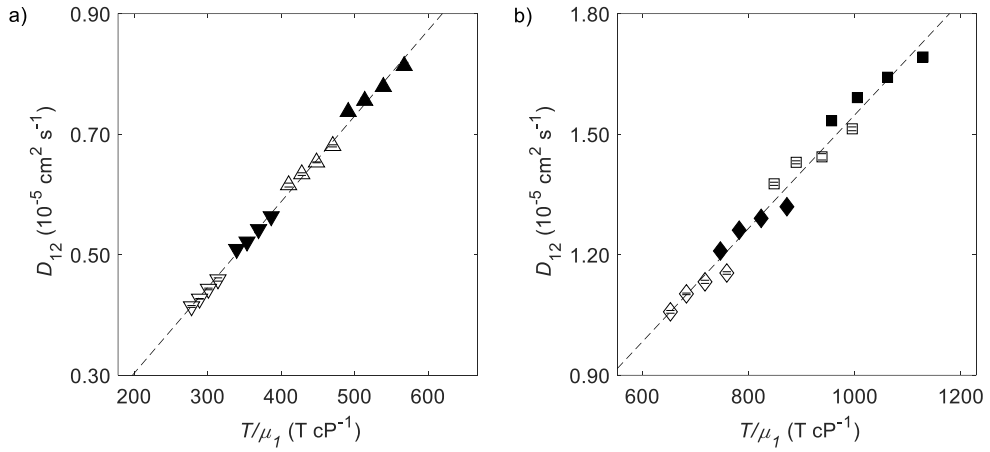

Figure 4 – D_{12} values *versus* Stokes-Einstein abscissas (T/μ_1) for quercetin in a) liquid ethanol and in b) liquid ethyl acetate for temperatures of 303.15 K (▽ and ◇), 313.15 K (▼ and ◆), 323.15 K (△ and □) and 333.15 K (■ and ▲).

4.3 Modeling results

Eleven equations were tested for systems in study, EtOH/quercetin and EtOAc/quercetin, as mentioned in Section 2.2. The models performance was assessed in terms of AARD, the properties of the pure compounds required for the modeling can be found in Table 3 and the main results are shown in Table 4.

241 Table 3 – Properties of the chemical compounds studied in this work.

Compound	M_i (g mol^{-1})	P_c (bar)	T_c (K)	V_c (cm^3 mol^{-1})	T_b (K)	w	σ_{LJ} (Å)	ε_{LJ}/k_B (K)
Quercetin	302.24[a]	66.63[d]	1468.74[d]	730.5[d]	1187.6[c]	-	6.17951[e]	1136.80[e]
Ethanol	46.07[a]	61.40[d]	513.9[d]	167.1[d]	351.80[d]	0.677[d]	4.23738[f]	1291.41[f]
Ethyl acetate	88.11[a]	38.80[b]	523.30[b]	286.0[b]	350.21[d]	0.361[c]	5.31476[e]	405.03[e]

242 [a] Taken from safety data sheet; [b] Taken from Yaws [53]; [c] Estimated through the Joback's method [43]; [d] Taken from Reid *et al.* [43]; [e] Estimated by Equations 7 and 8 from Liu *et al.* [45]; [f] Taken
243 from Liu and Silva [38];

244 Table 4 – Modelling results for D_{12} of quercetin in ethanol and ethyl acetate: fitted parameter and average absolute deviation (AARD) for each model tested.

Model	No. of parameters	Ref.	EtOH/quercetin Parameters	AARD (%)	EtOAc/quercetin Parameters	AARD (%)
DHB	2	[38–40]	$B_{DHB} = 7.791 \times 10^{-8}$ mol cm^{-1} s^{-1}K$^{-0.5}$ $V_D = 55.15$ cm^3 mol^{-1}	4.76	$B_{DHB} = 5.738 \times 10^{-8}$ mol cm^{-1} s^{-1}K$^{-0.5}$ $V_D = 87.26$ cm^3 mol^{-1}	1.35

			$B_{\mathrm{DHB}} = 3.415 \times 10^{-8}$ mol cm^{-1} s^{-1}K$^{-0.5}$		$B_{\mathrm{DHB}} = 4.308 \times 10^{-8}$ mol cm^{-1} s^{-1}K$^{-0.5}$	
DHB & $V_{\mathrm{D}}(T)$	3	[38–41]	$m_{\mathrm{VD}} = -9.907 \times 10^{-2}$ cm^3 K mol^{-1}	0.79	$m_{\mathrm{VD}} = -5.423 \times 10^{-2}$ cm^3 K mol^{-1}	0.48
			$b_{\mathrm{VD}} = 8.123 \times 10^{1}$ cm^3 mol^{-1}		$b_{\mathrm{VD}} = 1.001 \times 10^{2}$ cm^3 mol^{-1}	
TLSM	0	[38,45,46]	-	51.79	-	7.41
TLSM$_{\mathrm{d}}$	1	[38,45,46]	$k_{12,\mathrm{d}} = -0.2422$	5.48	$k_{12,\mathrm{d}} = 3.534 \times 10^{-2}$	3.82
LJ-1	1	[47]	$k_{12,\mathrm{LJ}-1} = -0.8663$	8.84	$k_{12,\mathrm{LJ}-1} = -0.2131$	0.50
Wilke-Chang	0	[42,43]	-	40.60	-	48.53
Hayduk and Minhas	0	[44]	-	33.52	-	10.72
Empirical and semi-empirical correlations of Magalhães *et al.*	2	Eq. 3 of [48]	$a_3 = -0.9665$ $b_3 = -18.03$	0.98	$a_3 = -0.8621$ $b_3 = -17.87$	1.76
	2	Eq. 5 of [48]	$a_5 = 5.350 \times 10^{-6}$ cm^2 cP s^{-1} $b_5 = -8.217 \times 10^{-7}$ cm^2 s^{-1}	1.74	$a_5 = 5.524 \times 10^{-6}$ cm^2 cP s^{-1} $b_5 = -1.390 \times 10^{-6}$ cm^2 s^{-1}	3.13

2	Eq. 7 of [48]	$a_7 = -3.072 \times 10^{-7}\ \mathrm{cm^5\ g^{-1}\ K^{-1}\ s^{-1}}$ $b_7 = 2.569 \times 10^{-7}\ \mathrm{cm^2\ K^{-1}\ s^{-1}}$	4.09	$a_7 = -3.212 \times 10^{-7}\ \mathrm{cm^5\ g^{-1}\ K^{-1}\ s^{-1}}$ $b_7 = 3.242 \times 10^{-7}\ \mathrm{cm^2\ K^{-1}\ s^{-1}}$	0.81
2	Eq. 9 of [48]	$a_9 = 8.940 \times 10^{-10}\ \mathrm{cm^5\ g^{-1}\ K^{-1}\ s^{-1}}$ $b_9 = 1.414 \times 10^{-8}\ \mathrm{cm^2\ cP\ K^{-1}\ s^{-1}}$	1.01	$a_9 = 6.027 \times 10^{-9}\ \mathrm{cm^5\ g^{-1}\ K^{-1}\ s^{-1}}$ $b_9 = 1.375 \times 10^{-8}\ \mathrm{cm^2\ cP\ K^{-1}\ s^{-1}}$	1.79

245

The AARD results in Table 4 show that, in general, both systems are well described by the selected models, with AARD spanning from 0.48 % to 51.79 %. As expected, the correlations achieve better performance than the predictive ones, this is specially evidenced when comparing the results between the TLSM and $TLSM_d$. The introduction of one adjustable parameter into the model decreases the AARD values from 51.79 % to 5.48 % for EtOH/quercetin and from 7.41 % to 3.82 % in the case of EtOAc/quercetin. In any case this could be expected in advance, as the TLSM expression was developed for Lennard-Jonnes systems, which is not the case of pairs of molecules where the solvent establishes strong hydrogen bonds. Regarding the empirical or semi-empirical correlations of Magalhães *et al.* all of them achieve good results, correlating well D_{12} in both systems and providing AARD values in the range from 0.81 – 4.09 %. The low deviations of Magalhães *et al.* correlations were expected since they have been extensively tested and successfully validated with a large database composed of polar and non-polar, symmetrical and asymmetrical, and small and large molecules [48]. The LJ-1 correlation also shows good behaviour, with AARD values of 8.81 % and 0.50 % for EtOH/quercetin and EtOAc/quercetin, respectively, even thought it was not initially devised for liquid polar solvents. Analyzing the two hydrodynamic equations, the Wilke-Chang model achieves a poor performance for predicting D_{12} for both systems (40.60 % and 48.53 %) while that of Hayduk and Minhas showed mildly performance for the EtOAc/quercetin system with a deviation of 10.72 % and a weaker performance for EtOH/quercetin, AARD = 33.52 %. In both Wilke-Chang and Hayduk and Minhas equations, the molar volume at normal boiling temperature was estimated by Tyn-Calus [65] relationship, which is generally applicable to most compounds except for some polar nitrogen and phosphorus molecules and low boiling permanent gases [43]. Finally, the DHB correlation achieves AARDs of 4.76 % and 1.35 % for EtOH/quercetin and

EtOAc/quercetin, respectively. These are good results specially if one takes into account that this model is frequently adopted to describe systems with negligible attractive forces. Furthermore, DHB model performance can be easily and significantly improved by expressing the minimum volume required for diffusion, V_{D}, as function of temperature, which causes the errors to decrease to 0.79 % and 0.48 % respectively. Nonetheless such improvement should be also attributed to the increased number of embodied parameters (three) in this case. Overall, one can recommend Equations 3 (or 9) and 7 from the original work of Magalhães *et al.* [48] to calculate the diffusivity of quercetin in ethanol and ethyl acetate, respectively. They are very simple, achieve AARDs lower than 1 %, and require only the solvent density, viscosity and temperature. Moreover, it was shown they possess good extrapolation ability [48].

One of the empirical and semi-empirical expressions of Magalhães *et al.* was selected to represent simultaneously the D_{12} values of both systems with the same set of parameters. It was possible to correlate D_{12} of a single solute in two distinct solvents by fitting a single hydrodynamic equation (Equation 5 below) to data. For the two studied systems, the equation achieved an overall AARD of 2.63 % and, individually, AARD = 2.35 % for EtOH/quercetin and 2.91 % for EtOAc/quercetin. A graphical representation is shown in Figure 5.

$$D_{12} = 1.610 \times 10^{-8} \frac{T}{\mu_1} - 4.612 \times 10^{-7} \quad (5)$$

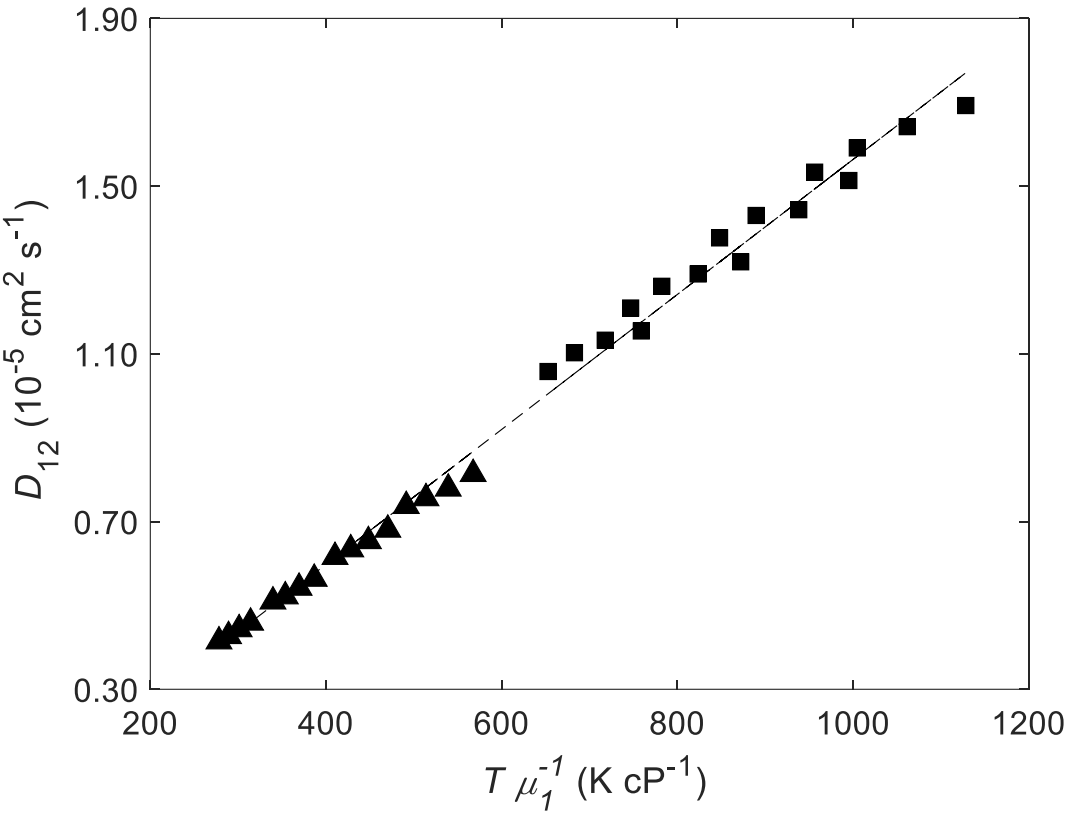

Figure 5 – D_{12} *versus* $T\ \mu_1{}^{-1}$ of quercetin in liquid ethanol (▲) and in liquid ethyl acetate (■). Symbols: experimental data; dashed line: Equation 5.

4.4 Effect of pressure on liquid diffusion

In 1984, Easteal [66] proposed the following equation to correlate self-diffusion, D_{11}, or tracer diffusion, D_{12}, coefficients in pressurized liquids with the system pressure:

$$\ln D_{12} = aP^{0.75} + b \tag{6}$$

where a and b are adjustable parameters. As a remark on the quality of this relation, in the original publication it was claimed that in many cases diffusion may be overestimated near the atmospheric pressure. In this work, this relation is tested not only with our data for quercetin, but also with D_{12} values published in previous works such as eucalyptol in ethanol [37] and squalene in ethyl acetate [41], and special attention is paid to the performance at lower pressures.

The adjusted data match the relation reported in the original article [66] and no deviation at lower pressures is found (see Figure 6) for the tested systems. In fact, these results are in accordance with the one reported in the original study for *n*-hexane where no deviations for temperatures between 298.15 K and 333.15 K were found, thought this is not true between 223.15 and 273.15 K for pressures under 500 bar. These observations suggest that the reported deviation might be not only pressure related but also temperature dependent. The resulting AARD of each studied system scored as low as 0.36 % for EtOH/eucalyptol, 0.35 % for EtOAc/squalene, 0.18 % for EtOH/quercetin, and 0.71 % for EtOAc/quercetin. It is important to mention that the low error benefits from the need to adjust new pairs of parameters to small sets of data, generally 3 or 4 experimental points. Nevertheless, Equation (5) seems to be valid for the investigated systems, which encompass polar to non-polar solutes, polar to weakly polar solvents, temperatures from 303.15 K to 333.15 K, and pressures from 1 bar to 150 bar.

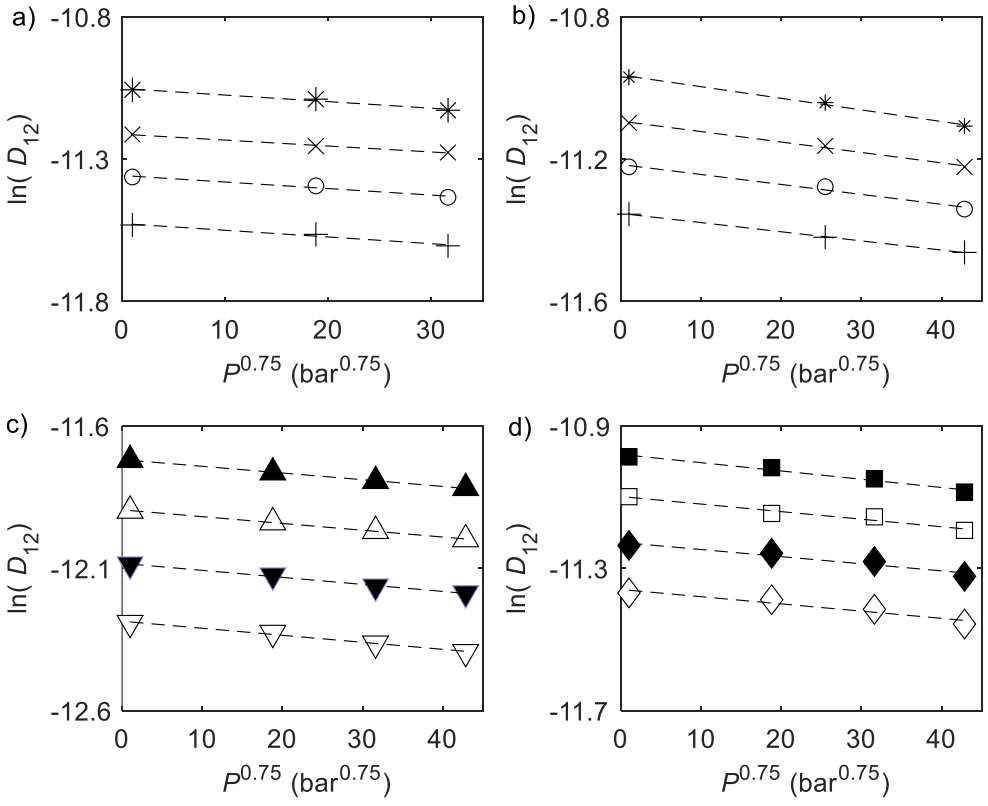

Figure 6 – Easteal [66] correlation results for: a) eucalyptol in ethanol taken from [58], b) squalene in ethyl acetate taken from [41], c) quercetin in ethanol from this work and d) quercetin in ethyl acetate from this work. Results are discriminated by temperature: – 303.15 K (+, ▽ and ◇), 313.15 K (◯, ▼ and ◆), 323.15 K (×, △ and □) and 333.15 K (✶, ■ and ▲).

4.5 D_{12} sensitivity on the accuracy of density and viscosity

In order to evaluate the tested models sensitivity to the accuracy of the solvent properties estimation method, ρ_1 (and naturally V_1) is calculated for both ethanol and ethyl acetate by the above mentioned equations (Tait, Eykman and Rackket) and also by the Peng-Robinson equation of state (PR EoS) [67]. In the particular case of ethanol, the viscosity calculation is density dependent, and thus the models sensitivity to viscosity is also tested. Accordingly, the average change in the ρ_1 value is of –6.54 % and reflects an average μ_1 decrease of –2.36 %. In turn, for ρ_1 of ethyl acetate, the difference is more subtle, being –3.51 % (in average). The values of μ_1 and ρ_1 calculated by the various methods for both solvents are compiled in Table A.1, presented as Appendix.

The diffusion coefficients of the four systems are modeled using the solvent density and viscosity calculated by the different methods (when applicable) in order to analyse the results. In terms of free-volume based models – (DHB correlation) - the four plots presented in Figure 7 allow a prompt identification of a non-random dispersion in at least one set of V_1 values of each system. This indicates that, for modeling purposes, the DHB free-volume model is very susceptible to the V_1 method of estimation. Furthermore, by analyzing Figure 7 and the AARD values shown in Table 5 one may further notice that the estimation of V_1 by the PR EoS equation improves the DHB equation results for ethanol systems (errors range from 2.67 % to 0.87 % for EtOH/eucalyptol, and from 4.76 % to 2.05 % for EtOH/quercetin). Nonetheless, for ethyl acetate systems the deviations

actually get worse (AARD scores from 0.69 % to 2.46 % for EtOAc/squalene and from 1.35 % to 3.27 % for EtOAc/quercetin).

With regard to the remaining considered models (TLSM, $TLSM_d$, Wilke-Chang and Hayduk and Minhas), the most sensitive one to the method of molar volume estimation is the TLSM, with the computed error increasing to an extra 70.47 % (EtOH/quercetin). This influence is easily mitigated inserting the $k_{12,\mathrm{d}}$ parameter in the diameter combining rule ($TLSM_d$ model), as illustrated in Figure 8. Furthermore, the said effect is not so persistent in hydrodynamic models with ethanol as solvent: the AARD differences only go from 0.92 % to 3.42 %. Finally, correlation models (DHB, DHB & $V_{\mathrm{D}}(T)$, $TLSM_d$, LJ-1 and Magalhães *et al.* expressions) led to minimal changes ranging from 0.02 % to 2.71 %, which demonstrates that the fitted parameters can accommodate the solvent density and viscosity calculation errors up to some degree. The exception is the non-random dispersion observed in the case of the DHB correlation as previously discussed in detail (see Figures 4 and 7).

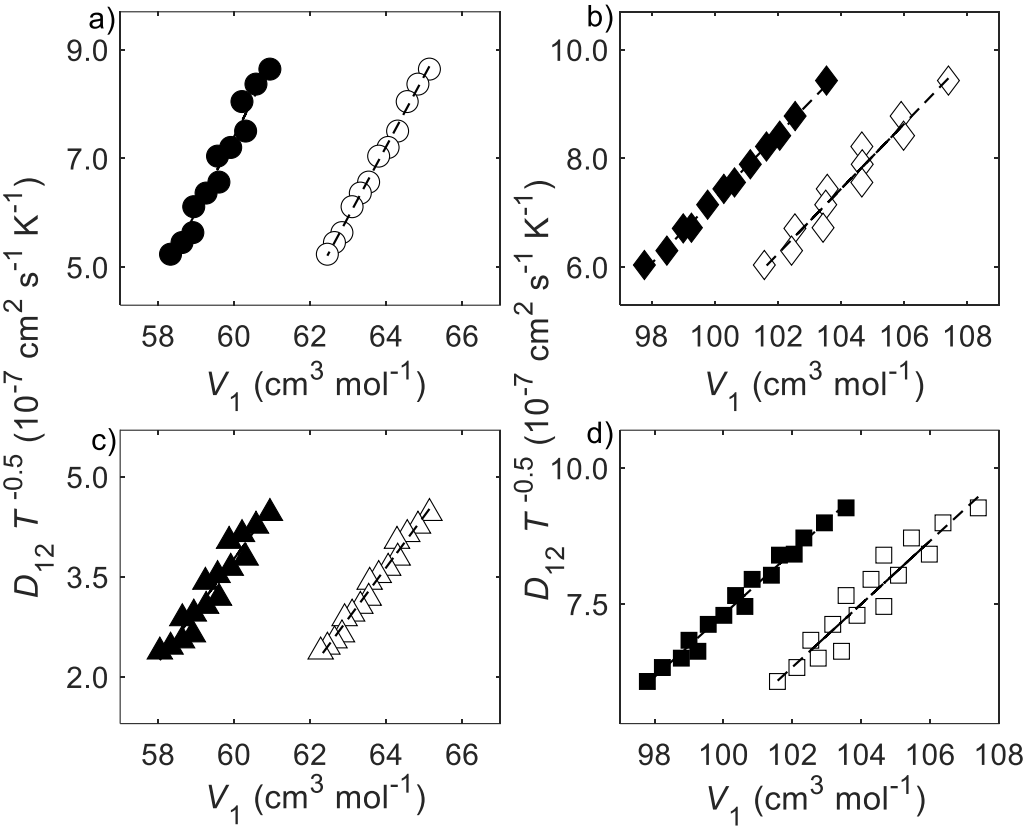

Figure 7 – $D_{12}T^{-0.5}$ *versus* solvent molar volume, V_1, for a) eucalyptol in ethanol, b) squalene in ethyl acetate, c) quercetin in ethanol and d) quercetin in ethyl acetate. Method of V_1 estimation discriminated by color: black symbols indicates V_1 estimated by either the Tai [49] and Eykman [50,51] equations (for EtOH (a) and (c)) or the Tait [49] and Rackett [53] equations (for ethyl acetate, (b) and (d)), and empty symbols indicates V_1 estimated by PR EoS [67]. Fitted results represented by (--).

362 Table 5 – AARD (%) values for each D_{12} model using V_1 values estimated by diferente equations (Tait [49], Eykman [50,51], Rackett [50] and PR EoS [67]).

Model		EtOH/eucalyptol		EtOH/quercetin		EtOAc/squalene		EtOAc/quercetin	
		Tait and Eykman	PR EoS	Tait and Eykman	PR EoS	Tait and Rackett	PR EoS	Tait and Rackett	PR EoS
DHB		2.67	0.87	4.76	2.05	0.69	2.46	1.35	3.27
DHB & $V_{\mathrm{D}}(T)$		0.63	0.33	0.79	0.47	0.50	0.36	0.48	0.53
TLSM		11.06	61.05	51.79	122.26	29.18	9.38	7.41	18.29
$\mathrm{TLSM_d}$		3.11	4.99	5.48	7.51	3.19	0.65	3.82	1.65
LJ-1		5.01	6.88	8.84	10.67	1.32	2.86	0.50	2.73
Wilke-Chang		28.76	27.58	40.60	44.02	-	-	-	-
Hayduk and Minhas		44.02	43.10	33.52	31.91	-	-	-	-
Magalhães *et al.*	Eq. 3 of [48]	0.42	1.00	0.98	0.69	-	-	-	-
	Eq. 5 of [48]	0.82	0.64	1.74	0.52	-	-	-	-
	Eq. 7 of [48]	2.14	0.56	4.09	1.62	0.58	1.64	0.81	2.47
	Eq. 9 of [48]	0.52	0.97	1.01	0.68	0.92	0.89	1.79	1.77

363

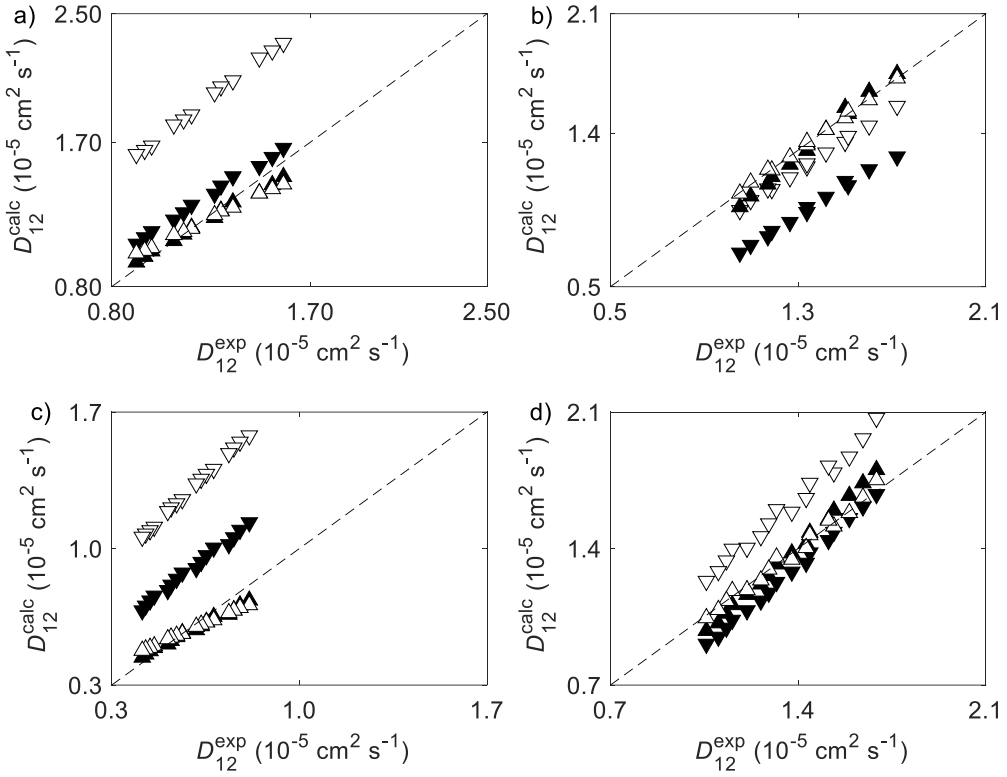

Figure 8 – Calculated *versus* experimental values of D_{12} calculated by the TLSM (▲) and TLSM$_d$ (▼) models for a) eucalyptol in ethanol, b) squalene in ethyl acetate c) quercetin in ethanol and d) quercetin in ethyl acetate. Method of V_1 estimation discriminated by: filled symbols indicate V_1 estimated by either the Tai [49] and Eykman [50,51] equations (for ethanol, (a) and (c)), or the Tait [49] and Rackett [53] equations (for ethyl acetate, (b) and (d)), and empty indicates V_1 estimated by the PR EoS [67].

5 Conclusions

The diffusivity (D_{12}) of quercetin is studied in two distinct liquid solvents, ethanol (EtOH) and ethyl acetate (EtOAc). The measurements are carried out using the CPB method at temperatures between 303.15 K and 333.15 K and pressures up to 150 bar. The D_{12} values for EtOH/quercertin are between 0.4142×10^{-5} and 0.8134×10^{-5} cm^{2}s^{-1} and for EtOAc/quercetin between 1.058×10^{-5} and 1.692×10^{-5} cm^{2}s^{-1}. The results

obtained for both systems were compared, showing that EtOAc/quercetin has higher D_{12} for equivalent conditions.

Modeling with eleven selected equations from the literature provide deviations between 0.79 % and 51.79 % for the EtOH/quercetin and between 0.48 % and 48.53 % for EtOAc/quercetin. Ultimately the best compromise between simplicity and low deviations is found to be Equations 3 (or 9) and 7 from Magalhães *et al.* for EtOH/quercetin and EtOAc/quercetin estimation, respectively. It is also shown it is possible to model both systems with a common set of parameters using one of the hydrodynamic based equations of Magalhães *et al*., which achieves an overall AARD of 2.63 %, and individual values of 2.35 % for EtOH/quercetin and 2.91 % for EtOAc/quercetin.

The pressure effect on D_{12} is evaluated, not only for the two systems measured in this work but also for two systems retrieved from the literature, EtOH/eucalyptol and EtOAc/squalene. The relation proposed by Easteal for pressurized liquids is tested showing it is valid for the four studied systems. Furthermore, the tested models dependency on the solvent density method of estimation is evaluated. The most D_{12} sensible model is found to be the Tracer Liu-Silva-Macedo (TLSM) where differences up to 70.47 % are noted. The smaller differences are found in correlation models, showing that the fitted parameters accommodate the errors related to the solvent property values.

Acknowledgments

This work was developed within the scope of the project CICECO-Aveiro Institute of Materials, UIDB/50011/2020 & UIDP/50011/2020, financed by national funds through the Portuguese Foundation for Science and Technology/MCTES. Bruno Zêzere thanks FCT for the PhD grant SFRH/BD/137751/2018.

401

402 ## Nomenclature and Acronyms

A_{peak}	Area of the chromatographic peak
AARD	Average absolute relative deviation
$Abs_{\max}$	Maximum absorbance of the peak
B_{DHB}	Interaction solute-solvent parameter in the DHB model
b_{VD}	Optimized parameter of the BHB & $V_{\text{D}}(T)$ model correlation
$\bar{C}(L,t)$	Average concentration of solute at column outlet
CPB	Chromatographic peak broadening
D	Dispersion coefficient defined by Equation 2
D_{12}	Tracer diffusion coefficient
D_{12}^{mix}	Diffusion coefficients in solvent mixtures
De	Dean number, $\text{De} = \text{Re}\sqrt{\zeta}$
DHB	Dymond-Hildebrand-Batchinski
EoS	Equation of state
EtOAc	Ethyl acetate
EtOH	Ethanol
H	Theoretical plate's high
L	Column length

LJ	Lennard-Jones
LJ-1	Hard sphere based model for D_{12} of real systems
m	Mass of a molecule
m_{VD}	Optimized parameter of the BHB & $V_{\mathrm{D}}(T)$ model correlation
M_{i}	Molecular weight of the component i
NAI	Normalized absorbance intensity
NDP	Number of data points
$k_{12,\mathrm{d}}$	Binary interaction constant of the $\mathrm{TLSM_d}$ correlation
$k_{12,\mathrm{LJ-1}}$	Adjustable binary parameter of the LJ-1 model
P	Pressure
PR	Peng-Robinson
R_0	Column inner radius
R_{c}	Column coil radius
Re	Reynolds number
S_{10}	Symmetry factor at 10 % of peak high
Sc	Schmidt number, $\mathrm{Sc} = \mu_1/(\rho_1 D_{12})$
SFE	Supercritical fluid extraction
t	Time
T	Absolute temperature

TLSM	Tracer Liu-Silva-Macedo
$\bar{u}$	Average linear velocity
V_1	Solvent molar volume
V_D	Minimum diffusion volume
V_f	Free volume

Greek letters

ε	Root mean square error
$\varepsilon_\mathrm{LJ}/\mathrm{k_B}$	Lennard Jones energy parameter
ζ	Curvature ratio
μ_1	Solvent viscosity
λ	Wavelength
ρ_1	Solvent density
σ_LJ	Lennard Jones molecular diameter
ω	Acentric factor

Subscripts

1	Solvent
2	Solute

12	Solute-Solvent pair
b	Normal boiling point calculation
c	Critical property

Superscripts

calc	Calculated
exp	Experimental

Appendix

The solvent density and viscosity values of ethanol and ethyl acetate estimated by the Peng-Robinson equation of state are presented in Table A.1.

Table A.1 – Density, viscosity and molar volume of ethanol (ρ_{EtOH}, μ_{EtOH} and V_{EtOH} respectively) and ethyl acetate density and molar volume (ρ_{EtOAc}, V_{EtOAc} respectively) calculated by the Peng-Robinson equation of state.

Temperature (K)	Pressure (bar)	ρ_{EtOH} (g cm^{-3})	μ_{EtOH} (cP)	V_{EtOH} (g cm^{-3})	ρ_{EtOAc} (g cm^{-3})	V_{EtOAc} (g cm^{-3})
303.15	1	0.7332	0.9645	62.83	0.8519	103.4
	50	0.7355	0.9883	62.64	0.8575	102.8
	75	-	-	-	0.8602	102.4
	100	0.7377	1.0118	62.45	0.8627	102.1
	150	0.7398	1.0346	62.27	0.8675	101.6
313.15	1	0.7251	0.8100	63.54	0.8419	104.7
	50	0.7276	0.8328	63.32	0.8482	103.9

	75	-	-	-	0.8512	103.5
	100	0.730	0.855	63.1	0.8540	103.2
	150	0.732	0.877	62.9	0.8593	102.5
	1	0.7165	0.6868	64.30	0.8314	106.0
	50	0.7193	0.7090	64.05	0.8385	105.1
323.15	75	-	-	-	0.8418	104.7
	100	0.7221	0.7310	63.80	0.8449	104.3
	150	0.7248	0.7523	63.56	0.8508	103.6
	1	0.7073	0.5872	65.14	0.8204	107.4
	50	0.7106	0.6090	64.83	0.8283	106.4
333.15	75	-	-	-	0.8320	105.9
	100	0.7137	0.6306	64.55	0.8355	105.5
	150	0.7167	0.6515	64.28	0.8419	104.7

References

[1] S.G. Dmitrienko, V.A. Kudrinskaya, V. V. Apyari, Methods of extraction, preconcentration, and determination of quercetin, J. Anal. Chem. 67 (2012) 299–311. https://doi.org/10.1134/S106193481204003X.

[2] M. Lesjak, I. Beara, N. Simin, D. Pintać, T. Majkić, K. Bekvalac, D. Orčić, N. Mimica-Dukić, Antioxidant and anti-inflammatory activities of quercetin and its derivatives, J. Funct. Foods. 40 (2018) 68–75. https://doi.org/10.1016/J.JFF.2017.10.047.

[3] D. Xu, M.J. Hu, Y.Q. Wang, Y.L. Cui, Antioxidant activities of quercetin and its

complexes for medicinal application, Molecules. 24 (2019) 1123. https://doi.org/10.3390/molecules24061123.

[4] A. Damianaki, E. Bakogeorgou, M. Kampa, G. Notas, A. Hatzoglou, S. Panagiotou, C. Gemetzi, E. Kouroumalis, P.-M. Martin, E. Castanas, Potent inhibitory action of red wine polyphenols on human breast cancer cells, J. Cell. Biochem. 78 (2000) 429–441. https://doi.org/10.1002/1097-4644(20000901)78:3<429::AID-JCB8>3.0.CO;2-M.

[5] M. Kampa, A. Hatzoglou, G. Notas, A. Damianaki, E. Bakogeorgou, C. Gemetzi, E. Kouroumalis, P.M. Martin, E. Castanas, Wine antioxidant polyphenols inhibit the proliferation of human prostate cancer cell lines, Nutr. Cancer. 37 (2000) 223–233. https://doi.org/10.1207/S15327914NC372_16.

[6] M. Yoshida, T. Sakai, N. Hosokawa, N. Marui, K. Matsumoto, A. Fujioka, H. Nishino, A. Aoike, The effect of quercetin on cell cycle progression and growth of human gastric cancer cells, FEBS Lett. 260 (1990) 10–13. https://doi.org/10.1016/0014-5793(90)80053-L.

[7] M.G.L. Hertog, E.J.M. Feskens, P.C.H. Hollman, M.B. Katan, D. Kromhout, Dietary antioxidant flavonoids and risk of coronary heart disease: the Zutphen Elderly Study, Lancet. 342 (1993) 1007–1011. https://doi.org/10.1016/0140-6736(93)92876-U.

[8] A.W. Boots, G.R.M.M. Haenen, A. Bast, Health effects of quercetin: From antioxidant to nutraceutical, Eur. J. Pharmacol. 585 (2008) 325–337. https://doi.org/10.1016/j.ejphar.2008.03.008.

[9] C. Prommuak, W. De-Eknamkul, A. Shotipruk, Extraction of flavonoids and carotenoids from Thai silk waste and antioxidant activity of extracts, Sep. Purif.

444 Technol. 62 (2008) 444–448. https://doi.org/10.1016/J.SEPPUR.2008.02.020.

445 [10] L.D. Kagliwal, S.C. Patil, A.S. Pol, R.S. Singhal, V.B. Patravale, Separation of
446 bioactives from seabuckthorn seeds by supercritical carbon dioxide extraction
447 methodology through solubility parameter approach, Sep. Purif. Technol. 80
448 (2011) 533–540. https://doi.org/10.1016/J.SEPPUR.2011.06.008.

449 [11] L. Huang, Y. Cao, G. Chen, Purification of quercetin in Anoectochilu roxburghii
450 (wall) Lindl using UMAE by high-speed counter-current chromatography and
451 subsequent structure identification, Sep. Purif. Technol. 64 (2008) 101–107.
452 https://doi.org/10.1016/J.SEPPUR.2008.07.021.

453 [12] S. Roy, S. Banerjee, T. Chakraborty, Vanadium quercetin complex attenuates
454 mammary cancer by regulating the P53, Akt/mTOR pathway and downregulates
455 cellular proliferation correlated with increased apoptotic events, BioMetals. 31
456 (2018) 647–671. https://doi.org/10.1007/s10534-018-0117-3.

457 [13] J. Pinela, M.A. Prieto, L. Barros, A.M. Carvalho, M.B.P.P. Oliveira, J.A. Saraiva,
458 I.C.F.R. Ferreira, Cold extraction of phenolic compounds from watercress by high
459 hydrostatic pressure: Process modelling and optimization, Sep. Purif. Technol. 192
460 (2018) 501–512. https://doi.org/10.1016/J.SEPPUR.2017.10.007.

461 [14] A. Wach, K. Pyrzyńska, M. Biesaga, Quercetin content in some food and herbal
462 samples, Food Chem. 100 (2007) 699–704.
463 https://doi.org/10.1016/j.foodchem.2005.10.028.

464 [15] K.L. Chiu, Y.C. Cheng, J.H. Chen, C.J. Chang, P.W. Yang, Supercritical fluids
465 extraction of Ginkgo ginkgolides and flavonoids, J. Supercrit. Fluids. 24 (2001)
466 77–87. https://doi.org/10.1016/S0896-8446(02)00014-1.

[16] S.M. Ghoreishi, A. Hedayati, S.O. Mousavi, Quercetin extraction from Rosa damascena Mill via supercritical CO_2: Neural network and adaptive neuro fuzzy interface system modeling and response surface optimization, J. Supercrit. Fluids. 112 (2016) 57–66. https://doi.org/10.1016/J.SUPFLU.2016.02.006.

[17] C.A.M. Afonso, J.G. Crespo, Green Separation Processes: Fundamental and Applications, Wiley-VCH, 2005.

[18] M.M.R. de Melo, I. Portugal, A.J.D. Silvestre, C.M. Silva, Environmentally Benign Supercritical Fluid Extraction, in: F. Pena-Pereira, M. Tobiszewski (Eds.), Appl. Green Solvents Sep. Process., Elsevier, 2017.

[19] R.B. Gupta, J.-J. Shim, Solubility in Supercritical Carbon Dioxide, CRC Press, NW, 2007.

[20] M.M.R. De Melo, A.J.D. Silvestre, C.M. Silva, Supercritical fluid extraction of vegetable matrices: Applications, trends and future perspectives of a convincing green technology, J. Supercrit. Fluids. 92 (2014) 115–176. https://doi.org/10.1016/j.supflu.2014.04.007.

[21] H. Li, S. Li, Y. Zhang, H. Duan, New supercritical fluid extraction treatment method for determination of tripterine in Tripterygium wilfordii Hook. F, J. Liq. Chromatogr. Relat. Technol. 31 (2008) 1422–1433. https://doi.org/10.1080/10826070802039382.

[22] T. Funazukuri, Concerning the determination and predictive correlation of diffusion coefficients in supercritical fluids and their mixtures, J. Supercrit. Fluids. 134 (2018) 28–32. https://doi.org/10.1016/j.supflu.2017.11.035.

[23] D. Prat, J. Hayler, A. Wells, A survey of solvent selection guides, Green Chem. 16

(2014) 4546–4551. https://doi.org/10.1039/c4gc01149j.

[24] R. Krishna, J.A. Wesselingh, The Maxwell-Stefan approach to mass transfer, Chem. Eng. Sci. 52 (1997) 861–911. https://doi.org/10.1016/S0009-2509(96)00458-7.

[25] R. Taylor, R. Krishna, Multicomponent mass transfer, in: Wiley Series in Chemical Engineering, John Wiley & Sons, Inc., New York, 1993.

[26] A. Vignes, Diffusion in binary solutions. Variation of diffusion coefficient with composition, Ind. Eng. Chem. Fundam. 5 (1966) 189–199. https://doi.org/10.1021/i160018a007.

[27] G. Taylor, Dispersion of soluble matter in solvent flowing slowly through a tube, Proc. R. Soc. A Math. Phys. Eng. Sci. 219 (1953) 186–203. https://doi.org/10.1098/rspa.1953.0139.

[28] G. Taylor, Diffusion and mass transport in tubes, Proc. Phys. Soc. Sect. B. 67 (1954) 857–869. https://doi.org/10.1088/0370-1301/67/12/301.

[29] G. Taylor, The dispersion of matter in turbulent flow through a pipe, Proc. R. Soc. A Math. Phys. Eng. Sci. 223 (1954) 446–468. https://doi.org/10.1098/rspa.1954.0130.

[30] R. Aris, On the dispersion of a solute by diffusion, convection and exchange between phases, Soc. R. 252 (1959) 538–550. https://doi.org/10.1098/rspa.1959.0171.

[31] T. Funazukuri, C.Y. Kong, S. Kagei, Impulse response techniques to measure binary diffusion coefficients under supercritical conditions, J. Chromatogr. A. 1037 (2004) 411–429. https://doi.org/10.1016/j.chroma.2004.03.043.

[32] T. Funazukuri, C.Y. Kong, S. Kagei, Infinite-dilution binary diffusion coefficients of 2-propanone, 2-butanone, 2-pentanone, and 3-pentanone in CO_2, Int. J. Thermophys. 21 (2000) 1279–1290. https://doi.org/10.1023/A:1006749309979.

[33] O. Levenspiel, W.K. Smith, Notes on the diffusion-type model for the longitudinal mixing of fluids in flow, Chem. Eng. Sci. 50 (1995) 3891–3896. https://doi.org/10.1016/0009-2509(96)81817-3.

[34] T. Funazukuri, C.Y. Kong, S. Kagei, Binary diffusion coefficients in supercritical fluids: Recent progress in measurements and correlations for binary diffusion coefficients, J. Supercrit. Fluids. 38 (2006) 201–210. https://doi.org/10.1016/j.supflu.2006.02.016.

[35] E.T. van der Laan, Notes on the diffusion type model for longitudinal mixing in flow, Chem. Eng. Sci. 7 (1958) 187–191.

[36] C.M. Silva, C.A. Filho, M.B. Quadri, E.A. Macedo, Binary diffusion coefficients of α-pinene and β-pinene in supercritical carbon dioxide, J. Supercrit. Fluids. 32 (2004) 167–175. https://doi.org/10.1016/j.supflu.2004.01.003.

[37] B. Zêzere, A.L. Magalhães, I. Portugal, C.M. Silva, Diffusion coefficients of eucalyptol at infinite dilution in compressed liquid ethanol and in supercritical CO_2/ethanol mixtures, J. Supercrit. Fluids. 133 (2018) 297–308. https://doi.org/10.1016/j.supflu.2017.10.016.

[38] H. Liu, C.M. Silva, Modelling of transport properties of hard sphere fluids and related systems and its applications, in: Lect. Notes Phys. 753 Theory Simul. Hard-Sph. Fluids Relat. Syst., Springer, Berlin/Heidelberg, 2008: pp. 37–109. https://doi.org/10.1007/978-3-540-78767-9_9.

[39] J.H. Dymond, Corrected Enskog theory and the transport coefficients of liquids, J. Chem. Phys. 60 (1974) 969–973. https://doi.org/10.1063/1.1681175.

[40] J.H. Dymond, E. Bitch, E. Vogel, W.A. Wakeham, V. Vesovic, M.J. Assael, Dense fluids, in: J. Millat, J.H. Dymond, C.A. Nieto de Castro (Eds.), Transp. Prop. Fluids. Their Correl. Predict. Estim., Cambridge University Press, Cambridge, 1996.

[41] B. Zêzere, J.M. Silva, I. Portugal, J.R.B. Gomes, C.M. Silva, Measurement of astaxanthin and squalene diffusivities in compressed liquid ethyl acetate by Taylor-Aris dispersion method, Sep. Purif. Technol. 234 (2020) 116046. https://doi.org/10.1016/J.SEPPUR.2019.116046.

[42] C.R. Wilke, P. Chang, Correlation of diffusion coefficients in dilute solutions, AIChE J. 1 (1955) 264–270. https://doi.org/10.1002/aic.690010222.

[43] B.E. Poling, J.M. Prausnitz, J.P. O'Connell, The Properties of Gases and Liquids, Fifth ed., The McGraw-Hill Companies, Inc, 2001.

[44] W. Hayduk, B.S. Minhas, Correlations for prediction of molecular diffusivities in liquids, Can. J. Chem. Eniineerinig. 60 (1982) 295–299. https://doi.org/10.1002/cjce.5450600213.

[45] H. Liu, C.M. Silva, E.A. Macedo, New equations for tracer diffusion coefficients of solutes in supercritical and liquid solvents based on the Lennard-Jones fluid model, Ind. Eng. Chem. Res. 36 (1997) 246–252. https://doi.org/10.1021/ie9602318.

[46] A.L. Magalhães, S.P. Cardoso, B.R. Figueiredo, F.A. Da Silva, C.M. Silva, Revisiting the liu-silva-macedo model for tracer diffusion coefficients of

supercritical, liquid, and gaseous systems, Ind. Eng. Chem. Res. 49 (2010) 7697–7700. https://doi.org/10.1021/ie1009475.

[47] A.L. Magalhães, F.A. Da Silva, C.M. Silva, New tracer diffusion correlation for real systems over wide ranges of temperature and density, Chem. Eng. J. 166 (2011) 49–72. https://doi.org/10.1016/j.cej.2010.09.069.

[48] A.L. Magalhães, P.F. Lito, F.A. Da Silva, C.M. Silva, Simple and accurate correlations for diffusion coefficients of solutes in liquids and supercritical fluids over wide ranges of temperature and density, J. Supercrit. Fluids. 76 (2013) 94–114. https://doi.org/10.1016/j.supflu.2013.02.002.

[49] M.J. Assael, J.H. Dymond, S.K. Polimatidou, Correlation and prediction of dense fluid transport coefficients, Fluid Phase Equilib. 15 (1994) 189–201. https://doi.org/10.1016/0378-3812(92)87021-E.

[50] J.J. Cano-Gómez, G.A. Iglesias-Silva, V. Rico-Ram-erez, M. Ramos-Estrada, K.R. Hall, A new correlation for the prediction of refractive index and liquid densities of 1-alcohols, Fluid Phase Equilib. 387 (2015) 117–120. https://doi.org/10.1016/j.fluid.2014.12.015.

[51] J.F. Eykman, Recherches réfractométriques (suite), Recl. Des Trav. Chim. Des Pays-Bas. 14 (1895) 185–202. https://doi.org/10.1002/recl.18950140702.

[52] J.J. Cano-Gómez, G.A. Iglesias-Silva, M. Ramos-Estrada, Correlations for the prediction of the density and viscosity of 1-alcohols at high pressures, Fluid Phase Equilib. 404 (2015) 109–117. https://doi.org/10.1016/j.fluid.2015.06.042.

[53] C.L. Yaws, Chemical Properties Handbook, First ed, McGraw-Hill Education, New York, 1998.

582 [54] D.S. Viswanath, T.K. Ghosh, D.H. Prasad, N.V.K. Dutt, K.Y. Rani, Viscosity of
583 liquids: theory, estimation, experiment, and data, Springer, Dordrecht, 2007.

584 [55] K. Lucas, Ein einfaches verfahren zur berechnung der viskosität von Gasen und
585 Gasgemischen, Chem. Ing. Tech. 46 (19874) 157–158.
586 https://doi.org/10.1002/cite.330460413.

587 [56] K.G. Joback, R.C. Reid, A unified approach to physical property estimation using
588 multivariate statistical techniques, Massachusetts Institute of Technology, 1984.

589 [57] K.G. Joback, R.C. Reid, Estimation of pure-component properties from group-
590 contributions, Chem. Eng. Commun. 57 (1987) 233–243.
591 https://doi.org/10.1080/00986448708960487.

592 [58] B. Zêzere, J. Cordeiro, J. Leite, A.L. Magalhães, I. Portugal, C.M. Silva,
593 Diffusivities of metal acetylacetonates in liquid ethanol and comparison with the
594 transport behavior in supercritical systems, J. Supercrit. Fluids. 143 (2019) 259–
595 267. https://doi.org/10.1016/J.SUPFLU.2018.06.003.

596 [59] T. Funazukuri, C.Y. Kong, S. Kagei, Infinite dilution binary diffusion coefficients
597 of benzene in carbon dioxide by the Taylor dispersion technique at temperatures
598 from 308.15 to 328.15 K and pressures from 6 to 30 MPa, Int. J. Thermophys. 22
599 (2001) 1643–1660. https://doi.org/10.1023/A:1013178614497.

600 [60] R. V. Vaz, A.L. Magalhães, A.A. Valente, C.M. Silva, Measurement and modeling
601 of tracer diffusivities of α-pinene in supercritical CO_2, and analysis of their
602 hydrodynamic and free-volume behaviors, J. Supercrit. Fluids. 107 (2016) 690–
603 698. https://doi.org/10.1016/j.supflu.2015.07.033.

604 [61] H. Liu, C.M. Silva, E.A. Macedo, Generalised free-volume theory for transport

properties and new trends about the relationship between free volume and equations of state, Fluid Phase Equilib. 202 (2002) 89–107. https://doi.org/10.1016/S0378-3812(02)00083-3.

[62] H. Liu, C.M. Silva, E.A. Macedo, Unified approach to the self-diffusion coefficients of dense fluids over wide ranges of temperature and pressure - hard-sphere, square-well, Lennard-Jones and real substances, Chem. Eng. Sci. 53 (1998) 2403–2422. https://doi.org/10.1016/S0009-2509(98)00036-0.

[63] C.M. Silva, H. Liu, E.A. Macedo, Models for self-diffusion coefficients of dense fluids, including hydrogen-bonding substances, Chem. Eng. Sci. 53 (1998) 2423–2429. https://doi.org/10.1016/S0009-2509(98)00037-2.

[64] C.M. Silva, E.A. Macedo, Diffusion coefficients of ethers in supercritical carbon dioxide, Ind. Eng. Chem. Res. 37 (1998) 1490–1498. https://doi.org/10.1021/ie970266n.

[65] M.T. Tyn, W.F. Calus, Estimating liquid molar volume, Processing. 21 (1975) 16–17.

[66] A.J. Easteal, A general empirical relationship between tracer or self-diffusion coefficients of liquids and pressure, AIChE J. 30 (1984) 641–642. https://doi.org/10.1002/aic.690300417.

[67] J.S. Lopez-Echeverry, S. Reif-Acherman, E. Araujo-Lopez, Peng-Robinson equation of state: 40 years through cubics, Fluid Phase Equilib. 447 (2017) 39–71. https://doi.org/10.1016/j.fluid.2017.05.007.